

On the Derivation of Young's Equation for Sessile Drops: Nonequilibrium Effects Due to Evaporation

Hans-Jürgen Butt,* Dmytro S. Golovko, and Elmar Bonaccorso

Max-Planck-Institute for Polymer Research, Ackermannweg 10, 55128 Mainz, Germany

Received: August 18, 2006; In Final Form: February 27, 2007

Sessile liquid drops have a higher vapor pressure than planar liquid surfaces, as quantified by Kelvin's equation. In classical derivations of Young's equation, this fact is often not taken into account. For an open system, a sessile liquid drop is never in thermodynamic equilibrium and will eventually evaporate. Practically, for macroscopic drops the time of evaporation is so long that nonequilibrium effects are negligible. For microscopic drops evaporation cannot be neglected. When a liquid is confined to a closed system, real equilibrium can be established. Experiments on the evaporation of water drops confirm the calculations.

1. Introduction

Consider a drop of liquid on a horizontal solid substrate. Viewed in profile the drop appears to meet the substrate at the line of three-phase contact under a certain angle, the contact angle Θ . In one of the most widely used equations of surface science the contact angle is related to the surface tensions of the liquid–vapor γ_L , solid–vapor γ_S , and solid–liquid interfaces γ_{SL} by

$$\gamma_L \cos \Theta = \gamma_S - \gamma_{SL} \quad (1)$$

This equation is attributed to Young.¹ Young's equation is the basis to quantify wetting phenomena. It can be derived by considering the surface tensions to be forces acting on the line of contact.^{1–4} In equilibrium their horizontal components must cancel each other out. In a sounder derivation the Helmholtz energy or the grand thermodynamic potential of the system is minimized,^{5,6} taking gravitation^{7–10} and a possible adsorption of dissolved substances^{7,11} into account.

Although Young's equation is one of the oldest and most used equations of physics and chemistry, it is in a rather delicate position scientifically, in that it is virtually impossible to prove experimentally^{12–14} and its theoretical derivation has generated significant and partially controversial discussion. It has been noted that Young's equation is a macroscopic equation, which does not concern itself with the liquid surface in close vicinity of the contact line.^{6,13,15,16} Surface forces between the solid and the liquid surfaces modify the shape of the liquid surface on the nanoscopic scale.^{15,17–22} As a result, the nanoscopic contact angle might be different from the optically observable macroscopic contact angle. This effect is restricted to typically 1–20 nm thick regions of the drop. It was further noted that for small drops a line tension, which is the free energy required to create three-phase contact line as an additional energy component, has to be added.^{13,15,21,23–25} It has been pointed out that mechanical deformation of the solid surface caused by the vertical component of the liquid surface tension and the Laplace pressure within the drop can modify the energy balance and change the contact angle for soft solid surfaces.^{3,26–30} A

severe limit of Young's equation is the fact that solid surfaces are usually not in thermodynamic equilibrium but that their structure and thus their surface tensions depend on the history of that particular solid surface. This and an often missing clear definition of which surface energy term enters in Young's equation has caused some confusion.^{7,31–34}

All the issues mentioned above limit the validity of Young's equation severely. This paper, however, deals with a different, fundamental aspect of Young's equation. Even ignoring all the issues mentioned above it is shown that Young's equation can only be derived in a strict thermodynamic way under conditions, which are experimentally almost never met. The reason is that a sessile drop is usually not in thermodynamic equilibrium because it will evaporate. Even in saturated vapor atmosphere it tends to evaporate because due to the curved liquid surface its vapor pressure is slightly higher than that of the vapor. In earlier derivations of Young's equation the exchange of material between the system and the outside world was neglected^{6,9,10,35} or the drop volume was assumed to be constant (as in refs 8, 9, 21, 29, and 36–39). For macroscopic drops this is a good assumption because evaporation only occurs on a time scale much longer than the observation time. For microscopic drops, however, evaporation effects are significant and the volume of the drop changes during a typical observation period. With the growing relevance of microfluidics and lab-on-chip technology these effects become more and more important.

In this paper we first clarify the boundary conditions under which Young's equation can be derived in a strict sense. Then we estimate the time constant for evaporation. Finally, we verify this estimation by experiments on drop evaporation. The aim of the experiments was to demonstrate that microdrops evaporate on a time scale of a typical contact angle experiment, even in saturated (or close to) atmosphere.

2. Theory

2.1. Boundary Conditions to Derive Young's Equation.

We consider the simple system of a pure liquid drop on a planar, homogeneous, inert, and undeformable solid surface (Figure 1). We neglect gravitation, which practically implies that the drop should be much smaller than the capillary constant $(2\gamma_L/\rho g)^{1/2}$; here ρ is the density of the liquid and $g = 9.81 \text{ m/s}^2$ is the standard acceleration of free fall. On the other hand we neglect

* Corresponding author. E-mail: butt@mpip-mainz.mpg.de. Fax: +49-6131-379-310. Phone: +49-6131-379-111.

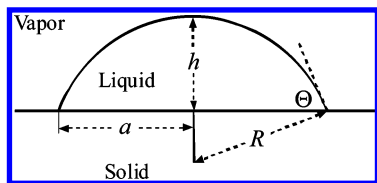


Figure 1. Schematic of a liquid drop on a solid surface in its vapor.

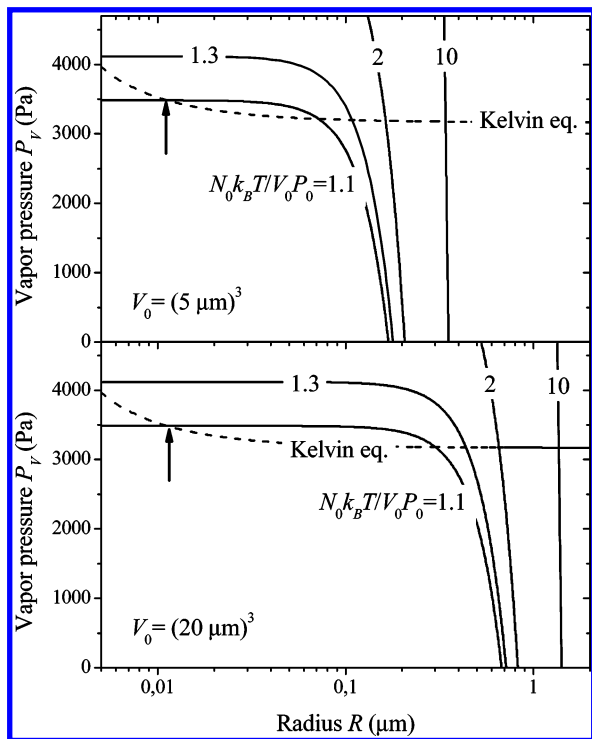


Figure 2. Vapor pressure calculated with Kelvin's equation (2) (dashed line) and with eq 8 (continuous) for water at 25 °C ($P_0 = 3169$ Pa, $\gamma_L = 0.072$ N/m) and volumes of $V_0 = 5 \mu\text{m}^3$ and $20 \mu\text{m}^3$. The number of molecules was set to $N_0 = 1.1, 1.3, 2.0$, and 10 times $P_0 V_0 / (k_B T)$. This leads to $N_0 = 1.06, 1.25, 1.92$, and 9.6×10^8 molecules, respectively, for $V_0 = 5 \mu\text{m}^3$ and 64 times as many molecules for $V_0 = 20 \mu\text{m}^3$. The arrows indicate an unstable radius.

line tension effects, and we do not take surface forces in the vicinity of the contact line into account. Practically, this implies that the drop should be much larger than $1 \mu\text{m}$. It is explicitly considered that molecules are exchanged between the liquid and the vapor phase. In equilibrium this is quantified by Kelvin's equation. To take equilibrium between the vapor and liquid phase into account, the thermodynamic boundary conditions have to be specified.

For an open system (temperature T , volume of the system V_0 , and chemical potential of the vapor μ_V are constant) equilibrium is established when the grand thermodynamic potential Ω is minimal. Toshev and Avramov²⁵ demonstrated that a sessile drop in an open system is not stable and will eventually evaporate. The physical mechanism leading to the instability is the exchange of molecules between the vapor and liquid phase, as expressed by the Kelvin equation

$$P_V = P_0 e^{\lambda/R} \quad \text{with} \quad \lambda = \frac{2\gamma_L V_m}{k_B T} \quad (2)$$

Here, P_0 is the vapor pressure of the liquid with a planar surface, R is the radius of curvature of the drop, V_m is the molecular volume in the liquid phase, k_B and T are Boltzmann's constant and temperature. The characteristic length scale in Kelvin's

equation λ for many liquids is $1\text{--}3$ nm (Table 1). It is important to note that the vapor pressure of the drop due to its curved surface is higher than P_0 . It has been pointed out that Young's equation is only valid in saturated vapor at pressure P_0 .^{14,31,32} Having a saturated vapor is, however, not sufficient. Oversaturation is required. An oversaturated vapor is thermodynamically not stable but will eventually condense to bulk liquid. As noted by Toshev and Avramov (and in contrast to the derivation in ref 40, p 380), in the presence of a drop as a nucleation center the vapor would immediately condense and be unstable.²⁵ Any small fluctuation of the radius R leads to an unstable situation. If R is coincidentally slightly larger than that given by Kelvin's equation, its vapor pressure would be lower than the actual external vapor pressure and the size of the drop will further increase. If R is coincidentally smaller than the equilibrium radius given by Kelvin's equation, it will completely evaporate.

This leads to two questions: First, can we derive Young's equation in a strict way by using different boundary conditions? Second, at which time scale can nonequilibrium effects be neglected?

Let us consider a closed system with constant V_0 , T , and a constant number of molecules N_0 . For a small number of molecules ($N_0 \leq P_0 V_0 / k_B T$) all molecules are in the vapor phase. A necessary requirement for drop formation is $N_0 > P_0 V_0 / k_B T$. Equilibrium is established when the Helmholtz energy change of the system

$$dF = (\gamma_{SL} - \gamma_S) dA_{SL} + \gamma_L dA_L - P_L dV_L - P_V dV_V + \mu_L dN_L + \mu_V dN_V \quad (3)$$

for any small change in the drop shape is zero. A_{SL} is the solid–liquid contact area and A_L is the area of the liquid–vapor interface. To derive eq 3 we used the fact that an increase in solid–liquid interfacial area is equal to the decrease in solid–vapor interfacial area. P_L , V_L , μ_L , and N_L are pressure, volume, chemical potential, and number of molecules of the liquid phase. The respective values for the vapor phase are P_V , V_V , μ_V , and N_V . For constant volume V_0 and constant number of molecules we have $dV_L = -dV_V$ and $dN_L = -dN_V$. Inserting

$$dF = (\gamma_{SL} - \gamma_S) dA_{SL} + \gamma_L dA_L - \Delta P dV_L + (\mu_L - \mu_V) dN_L \quad (4)$$

with $\Delta P = P_L - P_V$. In equilibrium, the chemical potentials of liquid and vapor are equal and the last term is zero. Choosing the drop height h and the contact radius a as independent variables describing the drop shape, we can write

$$A_{SL} = \pi a^2 \Rightarrow dA_{SL} = 2\pi a da \quad (5a)$$

$$A_L = \pi(a^2 + h^2) \Rightarrow dA_L = 2\pi a da + 2\pi h dh \quad (5b)$$

$$V_L = \frac{\pi}{6}(3a^2 h + h^3) \Rightarrow dV_L = \pi a h da + \pi h R dh \quad (5c)$$

In eq 5c we made use of the geometric relation $R = (a^2 + h^2)/(2h)$, where R is the radius of the hemispherical drop. Inserting this into eq 4 leads to

$$dF = \pi a [2(\gamma_{SL} - \gamma_S) + 2\gamma_L - h\Delta P] da + \pi h [2\gamma_L - R\Delta P] dh \quad (6)$$

TABLE 1: Vapor Pressure P_0 , Surface Tension γ_L (in 10^{-3} N/m), Diffusion Coefficients of the Vapor Molecules in Air (mostly taken from ref 50), Length Scale in Kelvin Equation (2) λ , Evaporation Times τ for Drops of $10 \mu\text{m}^3$ Initial Volume for 100% Vapor Pressure (eq 19) and 99% Vapor Pressure (eq 21), Critical Volume V_{cr} of Drops Assuming 100% Vapor Pressure (eq 19) and 99% Vapor Pressure (eq 21)^a

	P_0 (Pa)	γ_L (mN/m)	D (m ² /s)	λ (nm)	τ (s)		V_{cr} (mL)	
					100% P/P_0	99% P/P_0	100% P/P_0	99% P/P_0
water	3169	72.0	24×10^{-6}	1.04	741	10	0.0012	0.84
benzene	12700	28.2	9.3×10^{-6}	2.02	50	1.3	0.018	18
toluene	3790	27.9	8.5×10^{-6}	2.40	129	4.0	0.0070	3.3
acetone	30800	23.5	10.5×10^{-6}	1.40	32	0.58	0.028	61
diiodomethane	172	49.9	6.0×10^{-6}	3.26	3900	165	2.3×10^{-4}	0.013
trichloromethane	26200	26.7	8.9×10^{-6}	1.75	32	0.73	0.028	43
pentane	68300	15.6	8.4×10^{-6}	1.44	11	0.21	0.081	284
hexane	20200	17.9	7.3×10^{-6}	1.90	29	0.71	0.031	45
octane	1860	21.1	6.2×10^{-6}	2.79	203	7.4	0.0044	1.3
methanol	16900	22.1	15.2×10^{-6}	0.72	140	1.3	0.0064	18
ethanol	7870	22.0	11.8×10^{-6}	1.03	189	2.5	0.0048	6.6
1-propanol	2760	23.3	9.9×10^{-6}	1.41	366	6.3	0.0024	1.5
1-butanol	860	24.9	8.6×10^{-6}	1.84	851	20	0.0011	0.29
1-pentanol	259	25.4	7.2×10^{-6}	2.22	237	69	3.8×10^{-4}	0.048
1-hexanol	110	25.8	6.2×10^{-6}	2.61	4740	161	1.9×10^{-4}	0.013
1-octanol	10	27.1	5.1×10^{-6}	3.49	37800	1710	2.4×10^{-5}	3.8×10^{-4}
1,2-propanediol	20	40.1	8.8×10^{-6}	2.38	34600	1070	2.6×10^{-5}	7.7×10^{-4}
mercury	1.6×10^{-4}	486	14.2×10^{-6}	5.81	5.4×10^9	4.1×10^8	1.7×10^{-10}	3.3×10^{-12}

^a The critical volume is the volume of a drop evaporating in 15 min. Only for drops much larger than V_{cr} can evaporation be neglected for a typical observation time of 15 min. In all cases air at normal pressure and 25 °C and a contact angle of 60° was assumed.

Necessary conditions for a minimum in F are $\partial F/\partial h = 0$ and $\partial F/\partial a = 0$. The first condition leads to the Laplace equation

$$\Delta P = \frac{2\gamma_L}{R} \quad (7)$$

The second condition together with $\Delta P = 2\gamma_L/R$ and the geometric relation $\cos \Theta = 1 - h/R$ leads to Young's eq 1.

$\partial F/\partial a = \partial F/\partial h = 0$ are necessary but not sufficient conditions for stability. They only prove that F has an *extremum*, not necessarily a minimum. To argue that indeed in a closed system we have a stable situation, we consider thermal fluctuations of the drop size. If R is coincidentally larger than that given by Kelvin's equation, more molecules tend to condense. Then the vapor pressure decreases because N_V decreases and $N_0 = N_L + N_V$ is constant. Assuming the vapor to be an ideal gas we can express the vapor pressure by

$$P_V = \frac{N_V k_B T}{V_V} = \frac{(N_0 - N_L) k_B T}{(V_0 - V_L)} = \frac{N_0 V_m - V_L k_B T}{V_0 - V_L V_m} \quad (8)$$

To demonstrate real equilibrium, two conditions have to be fulfilled. First, the vapor pressures given by eqs 2 and 8 must be equal

$$\frac{N_0 V_m - V_L}{V_0 - V_L} \cdot \frac{k_B T}{V_m} = P_0 e^{\lambda/R} \quad (9)$$

Note that $V_0 > N_0 V_m > V_L$. We can express the liquid volume by the radius and contact angle $V_L = \pi R^3 \beta/3$ with $\beta = (2 + \cos \Theta)(1 - \cos \Theta)^2$. This determines R for a given volume of the system V_0 , amount N_0 , and contact angle (and thus β)

$$\frac{N_0 - \pi R^3 \beta/(3V_m)}{V_0 - \pi R^3 \beta/3} k_B T = P_0 e^{\lambda/R} \quad (10)$$

Unfortunately this is not an explicit expression. Graphically eq 10 can be illustrated by plotting the left- and right-hand sides in one graph (Figure 2). The left-hand side represents eq 8 while the right-hand side represents Kelvin's equation (2). In Figure

2 the vapor pressure of water is plotted versus the drop radius at 25 °C, a contact angle of $\Theta = 60^\circ$ ($\beta = 0.625$), two volumes of $V_0 = 5 \mu\text{m}^3$ and $20 \mu\text{m}^3$, and for different numbers of molecules N_0 . The equilibrium radius of a sessile drop can only be where the respective graphs cross each other.

The second condition for equilibrium is: At the radius R calculated with eq 10 the slope of the curve $P_V(R)$ given by eq 8 has to be steeper than the slope of $P_V(R)$ given by the Kelvin equation (2). Figure 2 demonstrates that this is indeed the case. This is essential because otherwise the drop would be unstable. An unstable situation arises, for example, for very small drops and low number of molecules N_0 . In Figure 2 this is indicated by an arrow at $R = 10$ nm and $N_0 = 1.1V_0 P_0/(k_B T)$. Then, eq 10 has two solutions but only the one at higher radius leads to a stable drop. That confinement can lead to a stabilization of droplets in an oversaturated vapor has already been realized for homogeneous nucleation.^{41–44} To our knowledge it was not extended to sessile drops and thus has not been related to Young's equation.

2.2. Time Scale of Quasi-Equilibrium: Evaporation. For an open system a sessile drop is never stable. It evaporates (for $P_V \leq P_0$) or we get complete condensation ($P_V > P_0$). This does, however, not completely spoil all experiments because the time scale of drop evaporation in most applications is longer than the typical observation time. Evaporation for macroscopic drops in still air is limited by the diffusion of molecules through a saturated vapor region around the drop.^{45,46} For constant contact angle evaporation and assuming constant temperature the change in liquid volume is described by⁴⁷

$$\frac{dV_L}{dt} = -2\pi D \frac{c_0 - c_\infty}{\rho} f\left(\frac{3V_L}{\pi\beta}\right)^{1/3} \quad (11)$$

with

$$f = \frac{1}{2} (0.00008957 + 0.6333\Theta + 0.116\Theta^2 - 0.08878\Theta^3 + 0.01033\Theta^4) \quad (12)$$

for $10^\circ \leq \Theta < 180^\circ$ and Θ (in radians). Here, D is the diffusion constant of vapor molecules in the gas phase, ρ is the density of the liquid, c_0 is the concentration of vapor molecules in direct vicinity to the liquid surface, and c_∞ is the concentration at infinite distance, both given in kg/m^3 . The concentration c_∞ is determined by the external vapor pressure and the molecular mass M by $c_\infty = MP_V/k_B T$. The concentration c_0 is determined by the vapor pressure as given by Kelvin's equation

$$c_0 = \frac{MP_0}{k_B T} e^{\lambda/R} \quad (13)$$

Assuming that the external vapor pressure is equal or close to the saturation vapor pressure, $P_V = (1 - x)P_0$, where $x \ll 1$, we get

$$c_0 - c_\infty = \frac{MP_0}{k_B T} (e^{\lambda/R} - 1 + x) \quad (14)$$

Since $R \gg \lambda$ we can write

$$\frac{c_0 - c_\infty}{\rho} = \frac{MP_0}{k_B T \rho} \left(\frac{\lambda}{R} + x \right) = \frac{P_0 V_m}{k_B T} \left(\frac{\lambda}{R} + x \right) \quad (15)$$

Inserting into eq 11 leads to

$$\frac{dV_L}{dt} = -2\pi D \frac{P_0 V_m}{k_B T} \left(\frac{\lambda}{R} + x \right) f \left(\frac{3V_L}{\pi\beta} \right)^{1/3} \quad (16)$$

Perfectly Saturated Vapor. Let us now consider the special case of perfectly saturated vapor ($x = 0$). Using $R = (3V_L/\pi\beta)^{1/3}$ we have

$$\frac{dV_L}{dt} = -2\pi D \frac{P_0 V_m \lambda}{k_B T} f \quad (17)$$

This can be integrated

$$V_L = V_{L0} - 2\pi D \frac{P_0 V_m \lambda}{k_B T} f t \quad (18)$$

Here, V_{L0} is the initial drop volume. The evaporation time τ of the drop is given by

$$\tau = \frac{1}{2\pi} \frac{V_{L0}}{D} \cdot \frac{k_B T}{P_0 V_m \lambda f} \quad (19)$$

The last factor depends on material properties of the system, namely, the saturation vapor pressure, the molecular volume, the contact angle (in f), and on the surface tension of the liquid (in λ). The time constant increases linearly with the initial volume of the drop. For this reason the relative size V_L/V_{L0} of large drops decreases slower than the relative size of small drops. Since the external vapor pressure cannot exceed P_0 , at least not in real thermodynamic equilibrium, τ given by eq 19 is the longest possible lifetime of a drop assuming constant contact angle evaporation. Equation 19 can also be rearranged. Assuming that a typical observation time is given, the size of a drop which will evaporate in that time can be calculated. Practically drops should be much larger than this size. For $\tau = 15$ min, values for the size of drops are given in the last two rows of Table 1.

As an example, Figure 3A shows τ versus the initial volume for the evaporation of sessile water drops with different contact angles. It relates the time and length scale where nonequilibrium

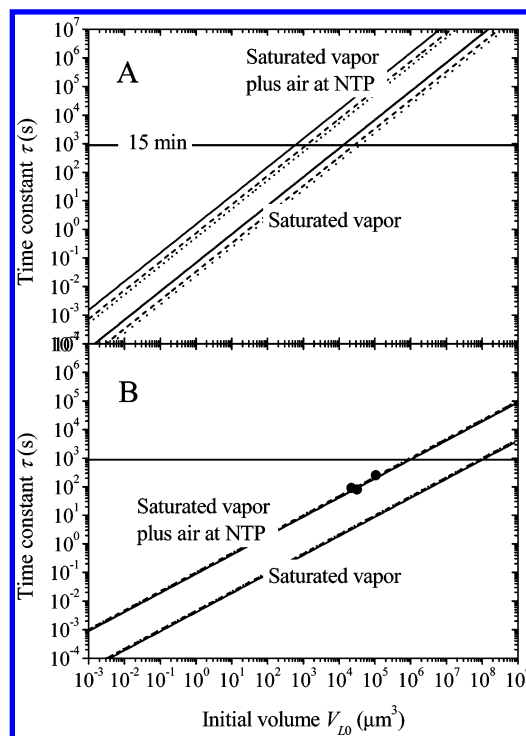


Figure 3. Time of evaporation of a sessile water drop at 25 °C versus the initial volume as calculated for 100% humidity with eq 19 (A) and for 99% humidity with eq 21 (B). Time constants were calculated for evaporation in the presence of air at normal pressure ($D = 2.4 \times 10^{-5} \text{ m}^2/\text{s}$) plus saturated water vapor and without background gas, only in a saturated vapor atmosphere ($D = 5.3 \times 10^{-4} \text{ m}^2/\text{s}$). The contact angles were assumed to be $\Theta = 30^\circ$ (continuous line), 60° (dashed), and 90° (dotted). The initial volume of the drop was varied from 100 nm^3 to 1 mm^3 . The times scale ranges from 0.1 ms to 116 days. The horizontal line indicates a typical observation time for a contact angle measurement of 15 min. For comparison, experimental results obtained for water drops evaporating from hydrophobized silicon cantilevers ($\Theta = 90^\circ$) are shown (●). These values were derived by extrapolating from the first 60 s of the evaporation process.

effects become significant. The top three curves were calculated for the typical situation of a water drop evaporating in air at normal pressure. For example a $10 \mu\text{m}^3$ sized water drop takes 741 s to evaporate. If we take 15 min as a typical observation time, we find that for $V_L > 0.0012 \text{ mL} = 10.6 \mu\text{m}^3$ evaporation can be neglected. Water drops smaller than this critical volume V_{cr} evaporate during the experiment. Only for drops much larger than this critical volume, we can neglect evaporation.

In the absence of a background gas, the diffusion coefficient is higher and evaporation is faster. From the viscosity of water vapor and assuming an ideal gas, the diffusion coefficient of water molecules in pure saturated vapor at $P_V = P_0 = 3169 \text{ Pa}$ can be calculated to be $D = 5.3 \times 10^{-4} \text{ m}^2/\text{s}$. In this case evaporation can only be neglected for drop volumes exceeding $50 \mu\text{m}^3$.

Not Perfect Saturation. Practically it is difficult to reach perfect saturation when measuring drop evaporation. To create a small drop, the system needs to have a small opening. In addition, temperature changes or differences somewhere in the system can create gradients in vapor pressure. In this case the parameter x in eq 15 can easily exceed λ/R . For example, even for 99% saturated vapor ($x = 0.01$) evaporation due to the unsaturated vapor will dominate for drops with typical $R \geq 0.1 - 0.2 \mu\text{m}$. Therefore we also calculated the time of evaporation for $x \gg \lambda/R$. Integrating eq 16 for negligible λ/R leads to

$$V^{2/3} = V_{L0}^{2/3} - \frac{4}{3} \pi D \frac{P_0 V_m}{k_B T} x f \left(\frac{3}{\pi \beta} \right)^{1/3} t \quad (20)$$

The evaporation time is

$$\tau = \frac{1}{4} \left(\frac{3}{\pi} \right)^{2/3} \frac{V_{L0}^{2/3}}{D} \frac{k_B T \beta^{1/3}}{P_0 V_m x f} \quad (21)$$

At 99% humidity (Figure 3B) we see three significant differences as compared to evaporation at perfect saturation:

Evaporation times are much faster. For example, a water drop of $100 \mu\text{m}^3$ volume is expected to evaporate in 140–400 h. At 99% humidity the evaporation time is only 800–1050 s.

The evaporation time increases proportional to $\tau \propto V_{L0}^{2/3}$ rather than $\tau \propto V_{L0}$. Thus, in the double-logarithmic plot the inclination of the graph is different.

The evaporation time depends less on the contact angle. At exactly 100% humidity, where evaporation is driven by the curvature of the liquid surface, the contact angle has a strong influence because it changes R .

The evaporation time and the critical volume for different liquids can be very different (Table 1). The main factor influencing the evaporation time is the vapor pressure P_0 of the molecules. Molecules which are large and interact strongly and thus have a low vapor pressure do not evaporate significantly on typical observation time scales. For example, in air and perfectly saturated vapor, a drop of $10 \mu\text{m}^3$ octanol or propanediol take ≈ 10 h to evaporate (in air at 100% saturated vapor). On the other hand, microdrops of acetone, trichloromethane, pentane, or hexane evaporate in less than 32 s, even in saturated vapor. If the relative vapor pressure is only 99% the evaporation times decrease by a factor 13–74. Thus, in any experiment, which takes longer than 1 min, the volume of the microdrop is likely to change significantly. The critical volume for evaporation in 99% relative vapor pressure increases by a factor of 50–700, and for many common liquids it exceeds 1 mL.

3. Experiment

3.1. Materials and Methods. To measure the time constant of evaporation, a water drop was placed in an atmosphere of saturated water vapor P_0 . To create a saturated water vapor the system contained a reservoir of water with a planar surface (Figure 4). Small drops were deposited onto hydrophobized microfabricated silicon cantilevers (rectangular cantilevers from Micromotive GmbH, Mainz, Germany) as described in ref 30. Drop evaporation was followed by imaging the shape of the liquid cap by an optical microscope. Cantilevers were only $90 \mu\text{m}$ wide so that the optical axis could be aligned with the plane of the cantilever. The drop shape was analyzed automatically with homemade software. Perfluoro-1,3-dimethylcyclohexane (Aldrich, 80% technical quality isomeric mixture) was deposited by plasma polymerization to form a hydrophobic film on the surface.⁴⁸ The thickness of the perfluorocarbon film was measured by ellipsometry and found to be 50 ± 3 nm. To create a saturated water vapor atmosphere in a closed system, we used a glass container (5×5 cm² base area, 1 cm high) covered at the top by Parafilm (Alcan Inc., Neehan, WI). The substrate was lifted ≈ 1 mm above a thin layer of water (deposited before the glass chamber is closed) at the bottom of the container. A large drop of ≈ 2 mm radius of curvature was placed directly underneath the cantilever.

Water (milliQ, Millipore Corp., USA) drops were generated by a computer-controlled piezoelectric drop generator⁴⁹ (Piezo-

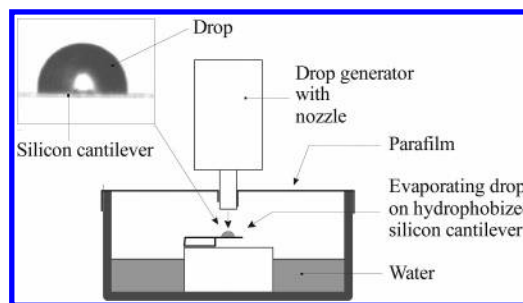


Figure 4. Experimental setup used to study evaporation of water drops in saturated water vapor atmosphere.

dropper, Universität Bremen, Germany). The nozzle of the drop generator was pushed through the Parafilm to a distance of ≈ 0.2 mm above the cantilever. By variation of the impulse duration and voltage applied to the piezoelectric drop generator, drops of different radii (15 – $36 \mu\text{m}$) and thus volume (14000 – $195000 \mu\text{m}^3$) could be produced. A three-axes, electromotor controlled micromanipulator (Luigs & Neumann GmbH, Ratingen, Germany) was used for controlling the nozzle-to-cantilever position. To visualize the process, the position and the contours of the drops on the cantilever were monitored with a camera system consisting of an objective $5\times$ (Mitutoyo Corp., Kawasaki, Japan), a $6.5\times$ Ultra zoom tube (Navitar Inc., Rochester, NY), and a uEye UI-2210-C, CCD camera (IDS GmbH, Obersulm, Germany), together with a white light source (Schott KL 1500, Mainz, Germany). The resolution of a single frame was 640×480 pixels, the frame rate was 1.5 frames/s. The light intensity was kept low to avoid heating of the sample, which would cause a local increase of the vapor pressure. From each frame of the video sequence, we calculated the contact radius a and the height h of the drop cap. To know the $\mu\text{m}/\text{pixel}$ ratio, the system was previously calibrated using a cantilever with a known length. From a and h , the drop volume was calculated by eq 5c. The drop deposition took place at a temperature of 21 ± 1 °C. Before the experiments were performed in a closed system in the presence of water, the level of relative humidity (RH) was measured with a humidity sensor (SHT15, Sensirion, www.sensirion.ch) with an accuracy of 2% specified in the range 10–90% RH. The RH was found to be 99%.

3.2. Results. A reproducible contact angle of $90 \pm 5^\circ$ was obtained for all the drops after deposition and in the beginning of evaporation. It was constant within at least half the evaporation time of the drop. The first part of the evaporation process followed the predicted evaporation law (eq 20) and $V_L^{2/3}$ decreased linearly with time. This demonstrates that the temperature changes caused by evaporating liquid are negligible. When this linear part is extrapolated to full evaporation, typical evaporation times ranged from 70 to 350 s. To a large part this variation is caused by the different initial volumes. The result obtained with 3 drops are plotted in Figure 5. For example drop 1 in Figure 5 evaporated within 5 min starting with an initial volume of $107.000 \mu\text{m}^3$. During the first 100 s it followed the evaporation law, i.e., $V_L^{2/3}$ decreases linearly with time. If we assume a diffusion coefficient of $D = 2.4 \times 10^{-5} \text{ m}^2/\text{s}$ for water in air at room temperature, take a contact angle of 90° ($f = 0.53$, $\beta = 2$), and use the experimental inclination of the graph $V_L^{2/3}$ versus time, we find from eq 20 a value for the humidity of 99.1% ($x = 0.009$). This agrees with the measured value of 99%. The same result is obtained if we use the evaporation of drop 3 for the first 60 s. The fact that the atmosphere seems to be not perfectly saturated is probably caused by tiny holes of the sealing of the Parafilm or in small temperature differences

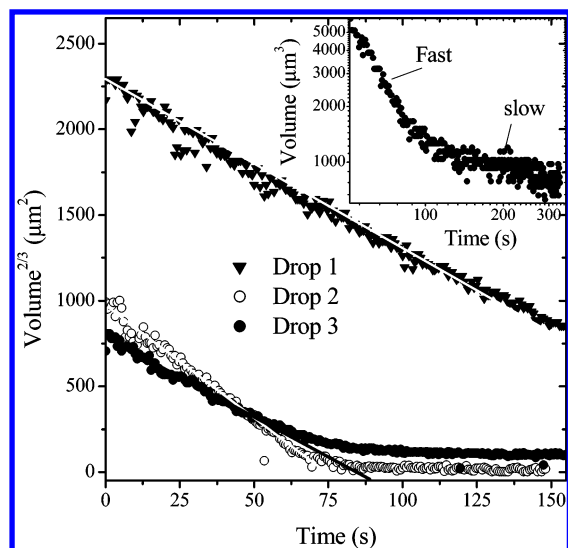


Figure 5. Change of volume of water drops V_L evaporating from hydrophobized silicon cantilevers in high (as high as possible) humidity. Results of three different experiments with three different drops are shown. Plotted is $V_L^{2/3}$, since this property is expected to decrease linearly with time (eq 20). The straight lines were used to extrapolate the evaporation time. Inset: V_L -versus-time on a double logarithmic scale.

across the vessel. For drop 2 a slightly lower humidity of 98.7% is calculated. In this case the nozzle of the dropper was shifted during the experiment and we believe that this caused a leak in the seal of the Parafilm around the nozzle.

In some cases, for example for drop 3, after an initial fast phase the evaporation process slowed down significantly and a slower phase of evaporation was observed (inset Figure 5). This led to long evaporation times of over 350 s, which cannot be explained by the fact that the contact angle changed during evaporation.

4. Conclusions

In an open system or for constant chemical potential of the vapor phase, a drop of a volatile liquid sitting on a hard, flat surface is never in thermodynamic equilibrium. Eventually it will evaporate. This is due to the fact that curved liquid surfaces possess an increased vapor pressure as compared to flat surfaces, as quantified by Kelvin's equation. Therefore it is not possible to derive Young's equation on thermodynamic grounds for open systems. This does not mean that Young's equation is invalid; it can just not be derived thermodynamically and the contact angle is not a thermodynamic quantity for a sessile drop. Only in a small, closed system a drop can be in thermodynamic equilibrium with its surrounding, and thus only for such a system it is possible to derive Young's equation.

For practical applications it is relevant to compare the time of evaporation with the duration of the experiment. The experiment is, for example, the measurement of a contact angle. If the time of the experiments is much shorter than the evaporation time, evaporation can be neglected and Young's equation can be used safely, even in an open system. Evaporation times for different liquids have been calculated assuming perfectly saturated vapor pressure and assuming 99% saturation. For water as an example, the evaporation time of a drop of 10 μm^3 from a surface with which it forms a contact angle of 60° initial volume cannot exceed 740 s, even at 100% RH. If the environment contains only 99% saturated vapor, the evaporation time is reduced by a factor of 13–74. Thus for microdrops Young's equation is of reduced significance.

For a given observation time we can define a critical drop volume. Only drops with a volume much larger than this critical volume show negligible evaporation. For drops smaller than this critical volume, evaporation effects are significant. We have shown that the critical volume of a drop depends on the properties of the liquid (saturation vapor pressure, molecular volume, and surface tension) and on the diffusion coefficient of its vapor in the background medium. We have discussed the case of a water droplet placed in saturated vapor with and without air as background medium. Evaporation is slowed down by air since its diffusion coefficient is reduced by a factor around 20. The fact that practically all contact angle experiments are carried out in the presence of air at normal pressure as a background gas established the significance of Young's equation.

Acknowledgment. We acknowledge helpful discussions with M. Deserno and M. Xuedan, help for depositing plasma polymer films from Jens Weinberg, and Masaya Toda for the film thickness characterization.

References and Notes

- (1) Young, T. *Philos. Trans. R. Soc. London* **1805**, 95, 65.
- (2) Freundlich, H. *Kapillarchemie*, 3rd ed.; Akademische Verlagsgesellschaft: Leipzig, 1923.
- (3) Kern, R.; Müller, P. *Surf. Sci.* **1992**, 264, 467.
- (4) Vafaei, S.; Podowski, M. Z. *Adv. Colloid Interface Sci.* **2005**, 113, 133.
- (5) Gibbs, J. W. *The Collected Works of J. Willard Gibbs, Thermodynamics*; Yale University Press: New Haven, CT, 1928; Vol. I.
- (6) Rusanov, A. I.; Shchekin, A. K.; Tatyankenko, D. V. *Colloids Surf., A* **2004**, 250, 263.
- (7) Johnson, R. E. *J. Phys. Chem.* **1959**, 63, 1655.
- (8) McNutt, J. E.; Andes, G. M. *J. Chem. Phys.* **1959**, 30, 1300.
- (9) Collins, R. E.; Cooke, C. E. *Trans. Faraday Soc.* **1959**, 55, 1602.
- (10) Everett, D. H. *Pure Appl. Chem.* **1980**, 52, 1279.
- (11) Johnson, A. E. *Colloids Surf., A* **2002**, 202, 33.
- (12) Jameson, G. J.; del Cerro, M. C. G. *J. Chem. Soc., Faraday Trans. I* **1976**, 72, 883.
- (13) White, L. R. *J. Chem. Soc., Faraday Trans. I* **1977**, 73, 390.
- (14) Adamson, A. W. *Physical Chemistry of Surfaces*; John Wiley & Sons: New York, 1990.
- (15) Churaev, N. V.; Starov, V. M.; Derjaguin, B. V. *J. Colloid Interface Sci.* **1982**, 89, 16.
- (16) de Gennes, P. G. *Rev. Mod. Phys.* **1985**, 57, 827.
- (17) de Feijter, J. A.; Vrij, A. *J. Electroanal. Chem.* **1972**, 37, 9.
- (18) Kralchevsky, P. A.; Ivanov, I. B. *Chem. Phys. Lett.* **1985**, 121, 116.
- (19) Indekeu, J. O. *Physica A* **1992**, 183, 439.
- (20) Toshev, B. V.; Avramov, M. Z. *Colloids Surf., A* **1995**, 100, 203.
- (21) Widom, B. *J. Phys. Chem.* **1995**, 99, 2803.
- (22) Solomentssev, Y.; White, L. R. *J. Colloid Interface Sci.* **1999**, 218, 122.
- (23) Pethica, B. A. *J. Colloid Interface Sci.* **1977**, 62, 567.
- (24) Boruvka, L.; Neumann, A. W. *J. Chem. Phys.* **1977**, 66, 5464.
- (25) Toshev, B. V.; Avramov, M. Z. *Colloids Surf., A* **1993**, 75, 33.
- (26) Lester, G. R. *J. Colloid Sci.* **1961**, 16, 315.
- (27) Rusanov, A. I. *Colloid J. USSR* **1977**, 39, 618.
- (28) Liu, Y.; German, R. M. *Acta Metall.* **1996**, 44, 1657.
- (29) White, L. R. *J. Colloid Interface Sci.* **2003**, 258, 82.
- (30) Bonaccorso, E.; Butt, H.-J. *J. Phys. Chem. B* **2005**, 109, 253.
- (31) Harkins, W. D.; Livingston, H. K. *J. Chem. Phys.* **1942**, 10, 342.
- (32) Melrose, J. C. *Adv. Chem. Ser.* **1964**, 43, 158.
- (33) Rusanov, A. I. *Surf. Sci. Rep.* **1996**, 23, 173.
- (34) Kwok, D. Y.; Neumann, A. W. *Colloids Surf., A* **2000**, 161, 31.
- (35) Li, T. *J. Chem. Phys.* **1962**, 36, 2369.
- (36) Gauss, C. F. Werke, 1830; Vol. 5; pp 31.
- (37) Bakker, G. Kapillarität und Oberflächenspannung. In *Handbuch der Experimentalphysik*; Wien, W., Harms, F., Eds.; Akademische Verlagsgesellschaft: Leipzig, 1928; Vol. VI; pp 458.
- (38) Lyklema, J. *Fundamentals of Interface and Colloid Science III*; Academic Press: San Diego, 2000.
- (39) Butt, H.-J.; Graf, K.; Kappl, M. *Physics and Chemistry of Interfaces*; Wiley-VCH: Berlin, 2003.
- (40) Rusanov, A. I. *Phasengleichgewichte und Grenzflächenerscheinungen*; Akademie-Verlag: Berlin, 1978.
- (41) Rao, M.; Berne, B. J.; Kalos, M. H. *J. Chem. Phys.* **1978**, 68, 1325.

- (42) Binder, K.; Kalos, M. H. *J. Stat. Phys.* **1980**, 22, 363.
- (43) Yang, A. J. M. *J. Chem. Phys.* **1985**, 82, 2082.
- (44) Peters, H.; Eggebrecht, J. *J. Phys. Chem.* **1991**, 95, 909.
- (45) Morse, H. W. *Proc. Am. Acad. Arts Sci.* **1910**, 45, 363.
- (46) Langmuir, I. *Phys. Rev.* **1918**, 12, 368.
- (47) Picknett, R. G.; Bexon, R. *J. Colloid Interface Sci.* **1977**, 61, 336.
- (48) Weber, A.; Pöckelmann, R.; Klages, C. P. *J. Vac. Sci. Technol., A* **1998**, 16, 2120.
- (49) Ulmke, H.; Wriedt, T.; Bauckhage, K. *Chem. Eng. Technol.* **2001**, 24, 265.
- (50) Lugg, G. A. *Anal. Chem.* **1968**, 40, 1072.